

2004

Monte Carlo simulations of exchange bias of ferromagnetic thin films on FeF₂ (110)

David Lederman

Ricardo Ramírez

Miguel Kiwi

Follow this and additional works at: https://researchrepository.wvu.edu/faculty_publications

Digital Commons Citation

Lederman, David; Ramírez, Ricardo; and Kiwi, Miguel, "Monte Carlo simulations of exchange bias of ferromagnetic thin films on FeF₂ (110)" (2004). *Faculty Scholarship*. 236.
https://researchrepository.wvu.edu/faculty_publications/236

This Article is brought to you for free and open access by The Research Repository @ WVU. It has been accepted for inclusion in Faculty Scholarship by an authorized administrator of The Research Repository @ WVU. For more information, please contact ian.harmon@mail.wvu.edu.

Monte Carlo simulations of exchange bias of ferromagnetic thin films on FeF₂(110)

David Lederman*

*Department of Physics, West Virginia University, Morgantown, West Virginia 26506-6315, USA*Ricardo Ramírez[†] and Miguel Kiwi*Facultad de Física, Pontificia Universidad Católica de Chile, Casilla 306, Santiago, Chile 6904411*

(Received 28 January 2004; revised manuscript received 4 June 2004; published 16 November 2004)

Monte Carlo simulations of hysteresis loops of FeF₂(110)/Fe bilayers were carried out. A large number of steps (360,000 steps/site) and a slow cooling schedule were implemented to ensure that quasi-equilibrium was reached at each temperature. The exchange bias field (H_E) at low temperature was calculated from the shift of the hysteresis loop center away from $H=0$. $H_E < 0$ was obtained for unequal exchange interactions between each antiferromagnetic sublattice and the ferromagnet. This puts forward a novel mechanism to break the spatial reversal symmetry, which is necessary to generate an exchange bias. Moreover, an effective perpendicular anisotropy was induced in the ferromagnet for large values of the interface exchange interactions. These results explain some of the reported experimental observations for FeF₂ exchange bias systems, both in thin-film and single-crystal forms, and are consistent with previous theoretical work.

DOI: 10.1103/PhysRevB.70.184422

PACS number(s): 75.70.Cn, 75.60.Ej, 75.30.Gw

I. INTRODUCTION

The phenomenon of exchange anisotropy has attracted much attention in recent years, both due to the basic challenge of developing a physical understanding of exchange anisotropy and to its application in magnetic sensor and magnetic media technology.^{1,2} The phenomenon is characterized by a shift of the center of the ferromagnetic hysteresis loop away from zero field by an amount known as the exchange bias field H_E . Exchange anisotropy is due to the magnetic interactions at the interface between a ferromagnet (FM) and an antiferromagnet (AF) or ferrimagnet. Recently, the antiferromagnet FeF₂ has been extensively investigated in this context, which provided important clues^{1,3} on the basic mechanism responsible for exchange bias (EB). Iron fluoride forms in the rutile tetragonal crystal structure. As a result of single-ion anisotropy and the anisotropic crystal-field, the Fe²⁺ ions experience a very strong uniaxial magnetic anisotropy along the [001] c -axis. In principle, this should simplify the data analysis, since there is a single AF easy-axis and thus the magnetic ordering at low temperatures should be unique. Nevertheless, some apparently contradictory data have been reported.⁴⁻⁷ For example, single-crystalline FeF₂(110) thin films with Co overlayers show that the coupling is along the in-plane [001] direction, which coincides with the effective magnetic anisotropy direction of the ferromagnetic film.^{4,5} In contrast, experiments with macroscopic FeF₂ single-crystals with Fe overlayers, have shown that the FM couples to the AF in a direction perpendicular^{6,7} to the c -axis (i.e., the [1 $\bar{1}$ 0] direction).

Recently Monte Carlo (MC) simulations of AF/FM bilayers have been performed to develop an understanding of exchange bias from a more fundamental point of view.⁸⁻¹¹ Some of this work^{8,9} was aimed at determining whether non-magnetic impurities in the AF can enhance EB, as has been observed experimentally.^{8,12} These experiments were performed on Co/Co_xMg_{1-x}O bilayers with a thin (0.4 nm)

layer of pure CoO at the interface, presumably to obtain identical interfaces, regardless of the Mg impurity concentration. On the other hand, the MC simulations^{8,9} were carried out for a system with a 50% dilute CoO monolayer ($x=0.5$) at the interface in order to induce, within the bulk of the antiferromagnet, a net exchange bias for all concentrations. This was done because the simulations assume a compensated antiferromagnetic surface (that is, two equivalent AF magnetic sublattices are present yielding a zero net moment). Having a pure layer at the interface, as in the experiments, would yield zero exchange bias. It is important to notice that previous experimental work on dilute Fe_xZn_{1-x}F₂ antiferromagnetic films with Co overlayers has also demonstrated that there is an enhancement of H_E , as long as the pure layer is deposited at the interface, but this enhancement disappears nontrivially (that is, it does not scale inversely with the film impurity concentration x) if the pure layer is not deposited at the interface.¹³ An additional complication is that the maximum exchange bias enhancement for Co/Co_xMg_{1-x}O bilayers occurs^{8,12} for $x=0.9$, whereas MC simulations find the peak at $x=0.4$. Therefore, it seems that MC simulations can yield qualitatively correct results, although important quantitative discrepancies remain which still need to be sorted out.

In this work we simulate FeF₂(110)/ferromagnetic bilayer films using MC simulations. The advantage of this system is that the easy axis is well defined (it is the [001] direction) and the exchange and anisotropy constants of FeF₂ are well known and hence it is an ideal candidate to test fundamental theories using the MC formalism. For example, FeF₂ has been used in the past to test finite-size scaling theories by comparing experimental data with MC simulations.¹⁴ In this paper we calculate the magnetic properties of the FM as a function of the interface exchange interaction. We demonstrate that we obtain $H_E \neq 0$, provided that the magnetic exchange coupling constants between the ferromagnet (FM) and the two antiferromagnetic (AF) sublattices are different.

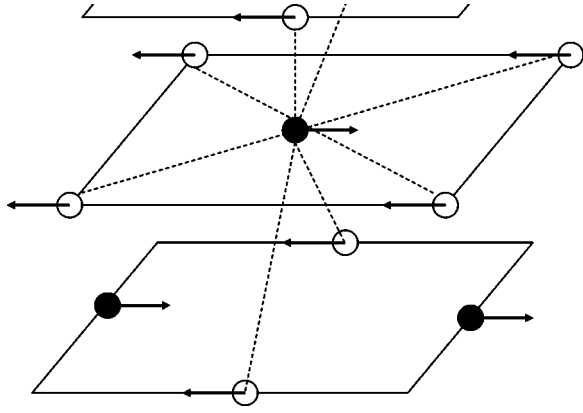


FIG. 1. Representation of the cells used for the simulations. The axes are indicated in the figure. The \circ and \bullet represent the two AF magnetic sublattices and the dotted lines indicate the nearest-neighbors. The magnetic spin ordering corresponds to the bulk AF at low T .

This constitutes a novel mechanism to break the spatial reversal symmetry, which is required to generate exchange bias.

The microscopic origin of the symmetry breaking mechanism that generates exchange bias is also an unresolved question. Recently Schulthess¹⁵ suggested that the Dzyaloshinsky-Moriya interaction¹⁶ is a possible symmetry breaking mechanism, and that for the $\text{Fe}_3\text{O}_4/\text{CoO}$ system it has the correct order of magnitude. In this contribution we find that an effective magnetic anisotropy is generated in the FM, for large values of AF/FM interface exchange constant. This is consistent with earlier theoretical work that demonstrated the existence of perpendicular coupling for compensated surfaces,^{17,18} although the strength of the interface exchange required for this to occur was not explored.

II. DESCRIPTION OF THE MODEL

Figure 1 illustrates the lattice geometry. The z -axis corresponds to the growth direction of (110) FeF_2 films, and the x -axis represents the FeF_2 [001] direction, which is also the easy axis of the AF. Notice that each (110) plane is fully compensated. The antiferromagnetic film was modeled by two $16 \times 16 \times 16$ interpenetrating sublattices. The FM had the same body-centered cubic structure as the AF, and its size was twice $16 \times 16 \times 4$. Periodic boundary conditions were established parallel to the x - y plane, with free boundary conditions along the z -axis, as illustrated in Fig. 1. The simulations were carried out using the importance sampling Metropolis algorithm and a checkerboard procedure that takes full advantage of the fact that only a nearest-neighbor exchange is assumed (no dipole interactions were taken into account).¹⁹ The calculations were carried out during 360,000 steps per site, discarding the first 280,000 and averaging the remainder to ensure proper thermalization.

A few runs were also made with 32×32 spins per sublattice in the x - y plane to verify that the results did not change the conclusions of this paper. For these larger lattices, the FM magnetization exhibited qualitatively less fluctuations

after more MC steps, but this did not alter qualitatively the relevant results.

The Hamiltonian for the system is

$$\begin{aligned} \mathcal{H} = & -J_{\text{AF}} \sum_{\langle i,j \rangle \in \text{AF}} \mathbf{S}_i \cdot \mathbf{S}_j - A \sum_{i \in \text{AF}} S_{ix}^2 - J_{\text{FM}} \sum_{\langle i,j \rangle \in \text{FM}} \mathbf{S}_i \cdot \mathbf{S}_j \\ & - g\mu_B \sum_{i \in \text{AF}} \mathbf{H} \cdot \mathbf{S}_i - g\mu_B \sum_{i \in \text{FM}} \mathbf{H} \cdot \mathbf{S}_i + J_{I1} \sum_{\langle i \in \text{AF}, j \in \text{FM} \rangle} \mathbf{S}_{i1} \cdot \mathbf{S}_j \\ & + J_{I2} \sum_{\langle i \in \text{AF}, j \in \text{FM} \rangle} \mathbf{S}_{i2} \cdot \mathbf{S}_j. \end{aligned} \quad (1)$$

The terms on the right-hand side represent the exchange interaction between AF spins, the AF uniaxial anisotropy, the exchange interaction between FM spins, the Zeeman interaction, and the exchange interaction between AF and FM spins at the interface, respectively. A is the anisotropy constant and J_{I1} and J_{I2} describe the exchange between the FM spins and the spins belonging to the first and second AF sublattice, respectively. All exchange interactions are between nearest neighbors only, denoted by $\langle \dots \rangle$ in the summations. Notice that no FM intrinsic anisotropy is included, which is a reasonable assumption because it is very small when compared to A and because the FM films grown on FeF_2 are usually polycrystalline. Hence, any anisotropy that appears in the FM must result from the interface exchange. In essence, the above model is a fully three-dimensional Heisenberg Hamiltonian with single-ion anisotropy in the antiferromagnet.

The parameters²⁰ used for the AF were those of bulk FeF_2 : $J_{\text{AF}} = -20.92$ K, $A = 37.13$ K, with $S_{\text{AF}} = 1$, where the spin is assumed to be a unit vector. Notice that in reality $S = 2$ for FeF_2 , so that J_{AF} is an effective exchange interaction that corresponds to the real J multiplied by S^2 . Also notice that the large anisotropy of FeF_2 could have allowed us to use a simpler Ising Hamiltonian for the antiferromagnet, as implemented for the simulations of the CoO system,⁹ but we wanted to investigate the possible formation of AF domain walls. Moreover, this procedure will also allow us to simulate, in the future, systems with lower anisotropy such as MnF_2 . The ferromagnetic spins are also unit vectors with an exchange $J_{\text{F}} = 200$ K, which is lower than the effective exchange in Fe or Co, but still significantly larger than J_{AF} . This made the ferromagnetic magnetization easier to reverse at low temperatures, lowering the coercive field. The exchange bias was determined as a function of J_{I1} and J_{I2} for $J_{I1} = J_{I2}$ and for $J_{I1} - J_{I2} = 5$ K. The latter case yields values of H_E comparable to those observed in real experiments with single-crystal FeF_2 thin films when scaled by the inverse of the FM thickness and the inverse of the FM magnetization.^{4,5} The difference between the two AF sublattices at the interface may be due to the direction of the F=Fe=F bonds which are different for the two sublattices. For one sublattice the bonds point out of the plane, while for the other it is in the plane.²¹ It is important to notice that this has nothing to do with extrinsic roughness. Steps on the surface, for example, would not alter this fact, because the inequality of the two sublattices is intrinsic and has to do with a difference in the symmetry of the fluorine ions, as shown in Fig. 2. This is true as long as the terraces are large enough so that interactions at step edges can be ignored.

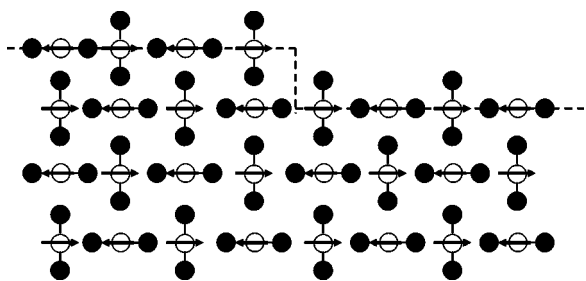


FIG. 2. Sketch of FeF_2 structure projected on $(1\bar{1}0)$ plane. The Fe^{2+} ions are represented by \circ and the F^{-} ions by \bullet . The dotted line represents the surface, including a monoatomic step. The arrows represent the low temperature magnetic configuration of FeF_2 , and also distinguish the two sublattices from each other. Notice that the sublattice with the Fe ions with spins pointing to the right have F ionic bonds pointing perpendicular to the surface, whereas the ones with spins pointing to the left have F bonds in the plane of the surface, regardless of the atomic step.

A major difficulty is encountered when attempting to find the lowest energy state, especially at low temperatures, because of the nature of the Heisenberg model. This manifests itself in very large coercivity values, making an accurate determination of H_E quite difficult. We addressed this issue via a two-pronged approach: (i) a very large number of time steps was used (360,000/site); and (ii) the sample was cooled in small temperature steps (5 K) in order to maintain thermal quasi-equilibrium during the cool-down procedure. This meant that for every single 5 K temperature step 360,000 steps/site (with the cooling field on) were performed in order to thermalize the sample. The sample was cooled from $T = 100$ K to $T = 20$ K. All hysteresis loops were computed at $T = 20$ K. Different cooling field values were investigated in the range between 0.01 T and 10 T. We found that the cooling field was not a significant factor in determining H_E

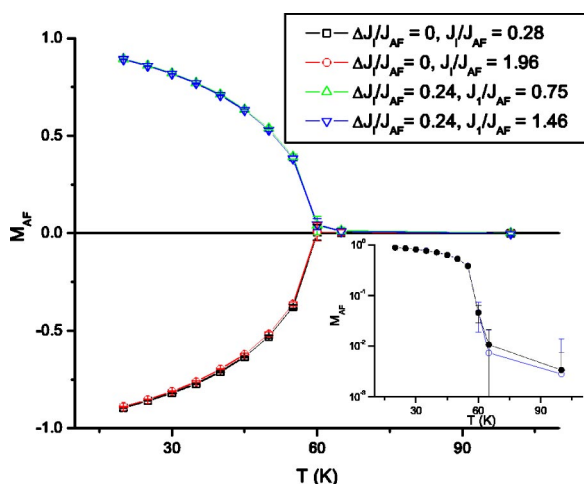


FIG. 3. Staggered magnetization of the antiferromagnet as a function of temperature. Here $\Delta J_I \equiv J_{I1} - J_{I2}$. M_{AF} is plotted in units of $g\mu_B = 1$. Inset: Semi-log graph of M_{AF} for samples with different lateral sizes, 16×16 (\bullet) and 32×32 (\circ), with the same thickness as all the other samples. Error bars correspond to standard deviation of the averaged M_{AF} measurements.

within our simple model. The data presented below were obtained with a 10 T cooling field applied along the $+x$ direction.

The uncertainty of the component of the magnetization along H, M_x , was estimated from the standard deviation of the values that were averaged to determine M_x . Near saturation ($M_x \sim 1$) the uncertainty was small, $\sigma(M_x) \approx 0.002$. In the regions where M_x approached zero, the uncertainty was much larger, of the order of $\sigma(M_x) \approx 0.04$. The latter uncertainty is approximately equal to the size of the symbols in Figs. 4 and 7 seen later.

The code was parallelized using the message-passing interface (MPI)²² implementations on an IBM SP at UCSD and the CRAY at IPICYT. The scalable library for pseudorandom number generation (SPRNG) was used to generate pseudorandom numbers in the parallel environment.²³ Since a checkerboard algorithm was used, each sublattice could be updated in parallel.

III. RESULTS AND DISCUSSION

A. Antiferromagnetic ordering

Figure 3 shows the value of the x -component of the staggered magnetization (order parameter) of the AFM ($M_{AF} = M_{1x} - M_{2x}$) as a function of temperature, as measured during the cool-down procedure. The change in sign of M_{AF} indicates that the antiferromagnetic configuration was reversed by 180° with respect to the positive values. We find that the Néel temperature is $T_N \sim 60$ K. This value is different from the known bulk FeF_2 Néel temperature²⁴ of $T_N = 78.4$ K. This discrepancy is not surprising given that our calculation is based on a classical Heisenberg Hamiltonian using a classical Monte Carlo procedure, which adds additional degrees of freedom that reduce the ordering temperature of the AFM. Also notice that for the case where a net interface coupling is present ($J_{I1} > J_{I2}$) T_N appears to be slightly enhanced, to perhaps as high a value as $T_N = 65$ K. Although the error bars do not permit a definite conclusion about this matter (and indeed this is not the main point of this paper), this is consistent with previous experimental²⁵ and Monte Carlo studies¹⁰ of exchange biased systems. In both the experimental and Monte Carlo results this was explained by the FM inducing long-range order on the AFM, above its decoupled Néel temperature T_N , when there is a net coupling with the ferromagnet.

B. $J_{I1} = J_{I2}$: Induced perpendicular coupling

When $J_{I1} = J_{I2} \equiv J_I$ our simulations reveal that there is no exchange bias ($H_E = 0$). Figure 4 illustrates the hysteresis loops of the FM as a function of J_I . Clearly, as J_I increases the loops become increasingly sheared. In experimental data this can be a consequence of an anisotropy perpendicular to the applied field. Because the y and z directions in our calculations are equivalent, the ferromagnet rotates uniformly either in the plane or out of the plane. Figure 5 is a graph of the magnitude of the component of M perpendicular to M_x , i.e., $M_{yz} = \sqrt{M_y^2 + M_z^2}$. Except for $J_I/J_{AF} = 0.28$, M_{yz} has no hysteresis and has a maximum near $H = 0$, clearly demon-

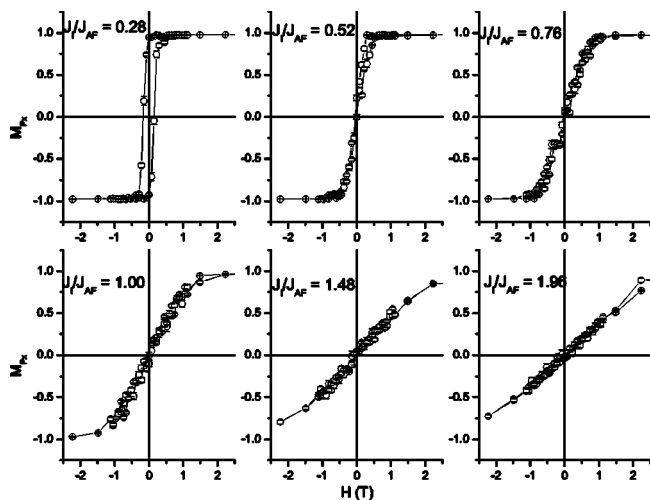


FIG. 4. x -component of the ferromagnetic magnetization vs the applied field, for $J_{I1}=J_{I2}\equiv J_I$. M_{F_x} is plotted in units of $g\mu_B=1$.

strating that in the vicinity of $H=0$ the magnetization is indeed perpendicular to the x -axis. For the $J_I/J_{AF}=0.28$ case there is significant hysteresis, and therefore there are two peaks in M_{yz} : one corresponding to the case where $M_x=0$ while decreasing the external field, and the other corresponding to the case where $M_x=0$ while increasing the field. In this case the induced perpendicular anisotropy is not strong enough to force the spins perpendicular to the x -axis at low fields.

Regarding the possibility of finding domain walls in either the antiferromagnet or ferromagnet, we notice that no domain walls were observed in the ferromagnet. This makes sense given that the intrinsic anisotropy of the ferromagnet in our model was set to zero, which results in an infinitely large domain wall, and that long-range dipolar interactions are also not taken into account. In the antiferromagnet we were able to observe, in one of our runs, the formation of a domain wall running parallel to the interface below the ferromagnet/antiferromagnet interface, only one unit cell wide. The small

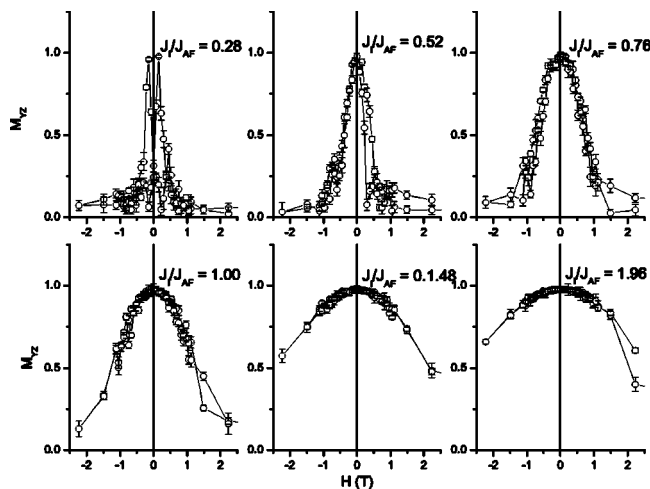


FIG. 5. Magnetization component of the ferromagnet perpendicular to the antiferromagnetic easy axis (x -axis) as a function of field for $J_{I1}=J_{I2}\equiv J_I$. The lines are guides to the eye.

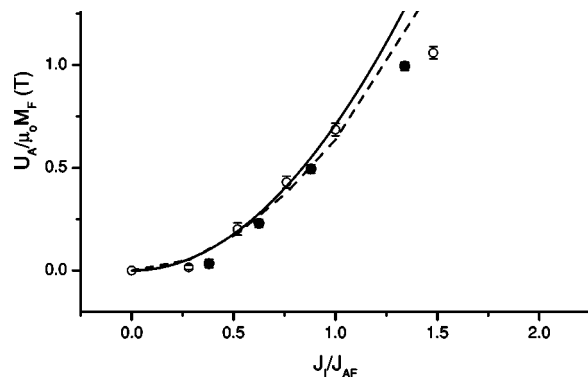


FIG. 6. Normalized effective anisotropy energy generated by the interface interaction as a function of the interface exchange energy $J_{I1}=J_{I2}\equiv J_I$ (\circ) and $J_{I1}-J_{I2}=5.0$ K, with $(J_{I1}+J_{I2})/2\equiv J_I$ (\bullet). The continuous line corresponds to Slonczewski's model with $M_F=M_{AF}=1$ and the dashed line to the same model but using the Monte Carlo-computed values of M_F and M_{AF} .

thickness of the domain wall is also expected from a calculation of the domain wall thickness, using $\delta=\pi\sqrt{A_{AF}/K_{AF}}$, where $A_{AF}=|J_{AF}|/a=20.92$ K/ a is the exchange stiffness and $K_{AF}=2A=74.26$ K/ a^3 the anisotropy energy, using the parameters for FeF_2 and taking into account a bcc crystal structure (2 atoms/unit cell), with a being the lattice constant. This leads to $\delta=1.7a$, so that the domain wall thickness is not expected to be much larger than one or two lattice spacings. However, the formation of the domain wall does not seem to affect the results relating to the magnetic response of the ferromagnet to an external field, perhaps because the large anisotropy in the antiferromagnet prevents the wall from being removed at low temperatures for the external fields used in our simulations. A relaxation of the domain wall would lead to a change in the sign of H_E because of the entire reversal of the antiferromagnetic moments at the interface. However, it is possible that relaxation of such a domain wall is important in other systems, such as those with magnetic impurities, where changes in the sign of H_E as a function of temperature have been observed.²⁶

It is possible to quantify the effective magnetic anisotropy energy $U_{A,\text{eff}}$ by the standard method of determining the missing area under the $M\cdot H$ curve,²⁷ such that (in SI units)

$$U_{A,\text{eff}} = \mu_0 \left(H_S M_S - \int_0^{H_S} M_x(H) dH \right), \quad (2)$$

where μ_0 is the permeability of free space, H_S is the field at which M_x saturates, and $M_S=M_F$ is the saturation magnetization. Figure 6 shows the result of such a calculation in units of the effective anisotropy field $H_{A,\text{eff}}\equiv U_{A,\text{eff}}/\mu_0 M_F$. The error bars in the figure are due to the uncertainty in determining H_S from Fig. 4. The effective anisotropy field appears to increase as J_I grows from zero and begins to saturate at a value of $J_I/J_{AF}\sim 1$.

This induced anisotropy makes sense in terms of the rapidly changing sign of the interface exchange $J_I S_{AF}$ at low temperatures from one interface antiferromagnetic site to the next. Slonczewski found analytically that an exchange inter-

action between two ferromagnetic layers that varies in space very rapidly, for example, for Fe layers separated by Cr with step disorder, results in biquadratic or perpendicular coupling between the layers.²⁸ This is because competing exchange interactions cause frustration, which leads to a perpendicular configuration as long as the spatial variation period of the exchange interaction is smaller than the domain wall thickness of the ferromagnet. The same idea can be applied to the antiferromagnetic/ferromagnetic bilayers simulated here. The interface ferromagnetic spins can also be divided into sublattices, each of which at low temperatures interacts with an antiferromagnetic sublattice. Therefore, it is possible to map the effective exchange at the interface onto a one-dimensional variation of the sign of the effective interface exchange along the y -axis because the AF sublattices point almost antiparallel to each other. Because of this, one can use Eq. (7) of Ref. 28 to calculate the effective perpendicular anisotropy energy. Specifically, the minimum energy per unit area is

$$U_A = -8^{-1} \sum_{\mathbf{k} \neq 0} (J_k/k)^2 (A_{AF}^{-1} \coth kt_{AF} + A_F^{-1} \coth kt_F) \sin^2(\bar{\theta}_{AF} - \bar{\theta}_F), \quad (3)$$

where J_k is a Fourier component of the effective interface exchange energy per unit area, \mathbf{k} is the Fourier component's wavevector, A_{AF} and A_F are the exchange stiffnesses of the antiferromagnet and ferromagnet, respectively, and t_{AF} and t_F are the thicknesses of the antiferromagnetic and ferromagnetic layers, respectively. In our case, $A_{AF(F)} = |J_{AF(F)}| M_{AF(F)}^2 / a$, taking into account the bcc lattice structure, and $\bar{\theta}_{AF(F)}$ are the average angles that the magnetization (or sublattice magnetization for the AF) makes with respect to the x -axis. In our case, the effective exchange interaction per unit area varies along the y -axis as $J_{I,\text{eff}} = 2J_I M_F M_{AF} \text{sgn}(\sin(2\pi y/a)) / a^2$, the factor of 2 coming from our bcc lattice structure where each ferromagnetic spin at the interface couples to two interface antiferromagnetic spins. We thus obtain a result similar to Eq. (9) in Ref. 28, namely that

$$U_A = \frac{4M_F^2 M_{AF}^2 J_{AF}^2}{\pi^3 a^2} \left(\frac{1}{M_F^2 |J_F|} \sum_{m=1}^{\infty} \frac{\coth[\pi(2m-1)2t_F/a]}{(2m-1)^3} + \frac{1}{M_{AF}^2 |J_{AF}|} \sum_{m=1}^{\infty} \frac{\coth[\pi(2m-1)2t_{AF}/a]}{(2m-1)^3} \right) \left(\frac{J_I}{J_{AF}} \right)^2. \quad (4)$$

(Notice that in the notation of Ref. 28, $U_A = 2|B_{12}|$ and $a = 2L$.) In our case, $t_F = 3a$ and $t_{AF} = 15a$ which makes the coth terms in the sums ≈ 1 . Since the first term in the series of Eq. (4) dominates, we have that

$$U_A = \frac{4M_F^2 M_{AF}^2 J_{AF}^2}{\pi^3 a^2} \left(\frac{1}{M_F^2 |J_F|} + \frac{1}{M_{AF}^2 |J_{AF}|} \right) \left(\frac{J_I}{J_{AF}} \right)^2. \quad (5)$$

To transform the biquadratic interface anisotropy energy U_A to an effective anisotropy field, we notice that the difference in energy per unit area in switching the ferromagnetic

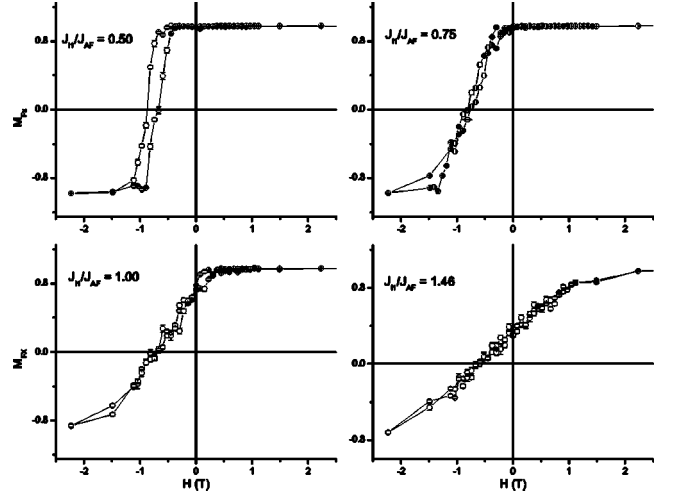


FIG. 7. The x component of the ferromagnet's magnetization as a function of the applied field for $J_{I1} - J_{I2} = 5$ K. M_F is in units of $g\mu_B = 1$.

magnetization by 90° from the x axis is $U_A = \mu_0 H_{A,\text{eff}} M_F t_F$. Using our values of $J_{AF} = -20.92$ K and $J_F = 200$ K, and $M_F = M_{AF} = 1$, the induced anisotropy field in Fig. 6 should vary as $H_{A,\text{eff}} = U_A / \mu_0 M_F t_F = C(J_I/J_{AF})^2$, with a prefactor $C = 0.95$ K = 0.71 T, assuming a g -factor equal to 2. The solid curve in Fig. 6 represents this result. If instead one uses the computed values of M_F and M_{AF} for each case, one obtains the slightly different result represented by the dashed line in Fig. 6. The agreement between the computational and analytical results is extremely good for small values of J_I/J_{AF} . For larger values of J_I/J_{AF} there is a significant discrepancy because the magnetization of the ferromagnet is strongly coupled to the antiferromagnetic sublattice magnetization, and hence Slonczewski's model is no longer valid.

C. $J_{I1} \neq J_{I2}$: Exchange bias

For the cases where $J_{I1} \neq J_{I2}$, $H_E \neq 0$. In Fig. 7 we show hysteresis loops for $\Delta J_I = J_{I1} - J_{I2} = 5$ K for different values of interface exchange J_{I1} . The exchange bias, as measured by the shift of the center of the hysteresis loops, appears to decrease slightly as J_{I1} is increased, as shown in Fig. 8.

It is interesting to compare this value with the effective exchange bias field assuming that it is only due to ΔJ_I . This is given by

$$H_E = \frac{\Delta J_I}{2t_F M_F \mu_0}. \quad (6)$$

With $t_F = 3$ unit cells, we have that $H_E = 0.64$ T, regardless of ΔJ_I , as illustrated by the dashed line in Fig. 8. Clearly this simple calculation gives the correct order of magnitude for H_E , although there is a slight dependence on ΔJ_I in the computational data. The origin of this effect may be a result of a subtle response of the ferromagnet and antiferromagnetic structure to the interface exchange, or it could be due to finite size effects. A further study is necessary to fully clarify this matter.

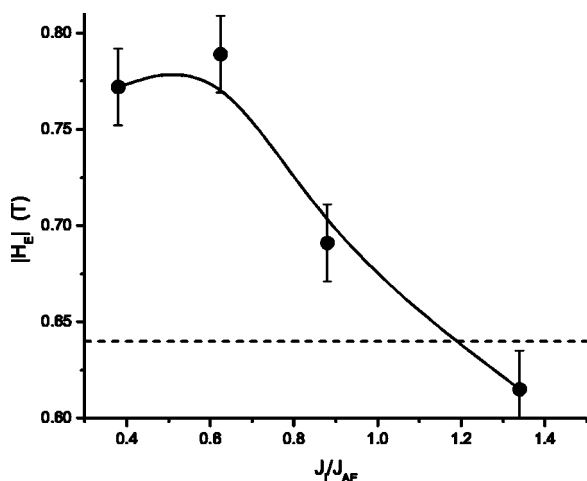


FIG. 8. Exchange bias field as a function of J_1/J_{AF} , where $J_1 = (J_{11} + J_{12})/2$. The dashed line represents the calculated H_E and the solid line is a guide to the eye.

As in the $J_{11} = J_{12}$ case, an increasing effective perpendicular magnetic anisotropy as J_{11} increases is also found for $J_{11} \neq J_{12}$. This is illustrated in Fig. 9, which shows the magnetization perpendicular to M_x as a function of H . The ferromagnetic spins clearly align themselves perpendicular to the antiferromagnetic easy axis near the $H = H_E$ value. The anisotropy can be determined using the same method as for the $J_{11} = J_{12}$ case. The results are shown in Fig. 6 with $(J_{11} + J_{12})/2 \equiv J_1$. These data agree well with the data obtained for the $J_{11} = J_{12}$ case. Hence, we conclude that the origin of the perpendicular anisotropy is the same in both cases.

IV. CONCLUSIONS

By implementing Monte Carlo simulations of the $\text{FeF}_2(110)$ /ferromagnetic bilayer system, we have demonstrated that exchange bias is generated when the AF sublattices have an unequal exchange coupling with the ferromagnet. The difference between the two coupling constants required to generate this anisotropic exchange can be quite small, i.e., $|J_{11} - J_{12}| \ll |J_{11}|$. Our MC simulations also demonstrate that the ferromagnet orders perpendicular to the in-plane [001] easy axis of the antiferromagnet for large values of interface exchange, regardless of whether or not there is unequal sublattice interface exchange. This is in agreement with previous theoretical calculations,^{29,30} although our simulations quantify the amount of exchange necessary for the perpendicular ordering to occur.

Our simulations may also settle contradictory data obtained from single crystals and epitaxial films.⁴⁻⁷ In (110)

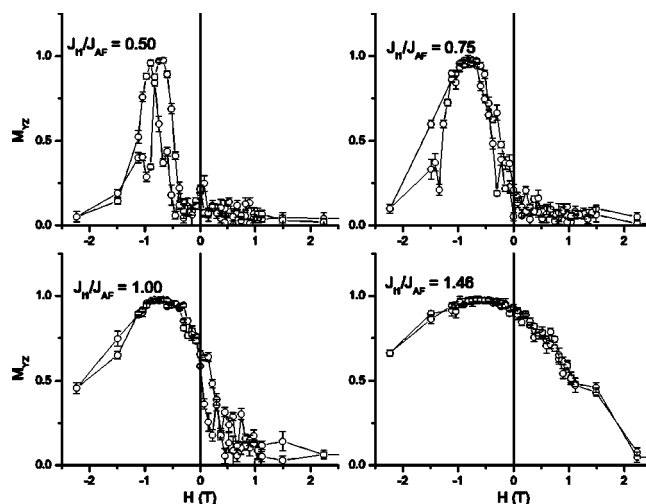


FIG. 9. Magnetization component of the ferromagnet perpendicular to the antiferromagnetic easy axis (x -axis) as a function of field for $J_{11} - J_{12} = 5$ K. The lines are guides to the eye.

FeF_2 single crystals, with thin Fe overlayers, a perpendicular anisotropy with little or no exchange bias has been observed at low temperatures,^{6,7} whereas in epitaxial single-crystal films with Co overlayers longitudinal anisotropy with a large exchange bias is observed.^{4,5} Our simulations indicate that this could be due to a stronger overall exchange between the antiferromagnet and the ferromagnet for the single crystal, which would result in the perpendicular anisotropy. The lack of exchange bias in the single crystal could be due to a very small (or zero) value of the difference $|J_{11} - J_{12}|$, whereas the opposite must occur in the films. While the first-principles reason for this is unclear, its cause may be related to surface reconstruction, small changes in the interface stoichiometry, or interface disorder. Additional interface structural data may be helpful in settling this issue.

ACKNOWLEDGMENTS

We gratefully acknowledge helpful discussions with Professor Aldo Romero of the Instituto Potosino de Investigación Científica y Tecnológica (IPICYT), México. Computing time was provided by the San Diego Supercomputer Center and the IPICYT. This work was performed while D.L. was on sabbatical leave at the Pontificia Universidad Católica de Chile in Santiago, partially funded by the Chilean Ministry of Education project MECESUP. Part of this work was done while Professor Ramírez was a visiting scholar at the University of California–San Diego, working in collaboration with Professor I. K. Schuller and funded by DOE. Part of the work at UCSD was also funded by NSF.

*Electronic address: David.Lederman@mail.wvu.edu

†Visiting fellow at UCSD.

- ¹J. Nogués and I. K. Schuller, *J. Magn. Magn. Mater.* **192**, 203 (1999), and references therein.
- ²A. E. Berkowitz and K. Takano, *J. Magn. Magn. Mater.* **200**, 552 (1999), and references therein.
- ³M. Kiwi, *J. Magn. Magn. Mater.* **234/235**, 584 (2001), and references therein.
- ⁴H. Shi and D. Lederman, *Phys. Rev. B* **66**, 094426 (2002).
- ⁵M. Grimsditch, A. Hoffmann, P. Vavassori, H. Shi, and D. Lederman, *Phys. Rev. Lett.* **90**, 257201 (2003).
- ⁶T. J. Moran, J. Nogués, D. Lederman, and I. K. Schuller, *Appl. Phys. Lett.* **72**, 617 (1998).
- ⁷M. R. Fitzsimmons, C. Leighton, J. Nogués, A. Hoffmann, K. Liu, C. F. Majkrzak, J. A. Dura, J. R. Groves, R. W. Springer, P. N. Arendt, V. Leiner, H. Lauter, and I. K. Schuller, *Phys. Rev. B* **65**, 134436 (2002).
- ⁸P. Miltényi, M. Gierlings, J. Keller, B. Beschoten, G. Güntherodt, U. Nowak, and K. D. Usadel, *Phys. Rev. Lett.* **84**, 4224 (2000).
- ⁹U. Nowak, K. D. Usadel, J. Keller, P. Miltényi, B. Beschoten, and G. Güntherodt, *Phys. Rev. B* **66**, 014430 (2002).
- ¹⁰S.-H. Tsai, D. P. Landau, and T. C. Schulthess, *J. Appl. Phys.* **93**, 8612 (2003).
- ¹¹O. Heinonen, *J. Appl. Phys.* **89**, 7552 (2001).
- ¹²J. Keller, P. Miltényi, B. Beschoten, G. Güntherodt, U. Nowak, and K. D. Usadel, *Phys. Rev. B* **66**, 014431 (2002).
- ¹³H. Shi, D. Lederman, and E. E. Fullerton, *J. Appl. Phys.* **91**, 7763 (2002).
- ¹⁴D. Lederman, C. A. Ramos, V. Jaccarino, and J. L. Cardy, *Phys. Rev. B* **48**, 8365 (1993).
- ¹⁵Y. Ijiri, T. C. Schulthess, J. A. Borchers, P. J. van der Zaag, and R. W. Erwin (unpublished).
- ¹⁶A. Crépieux and C. Lacroix, *J. Magn. Magn. Mater.* **182**, 341 (1998).
- ¹⁷N. C. Koon, *Phys. Rev. Lett.* **78**, 4865 (1997).
- ¹⁸T. C. Schulthess and W. H. Butler, *Phys. Rev. Lett.* **81**, 4516 (1998).
- ¹⁹D. P. Landau and K. Binder, *A Guide to Monte Carlo Simulations in Statistical Physics* (Cambridge University Press, Cambridge, 2000).
- ²⁰M. T. Hutchings, B. D. Rainford, and H. J. Guggenheim, *J. Phys. C* **3**, 307 (1969).
- ²¹M. Weissmann, A. M. Llois, and M. Kiwi, *J. Magn. Magn. Mater.* **234**, 19 (2001).
- ²²W. Gropp, E. Lusk, and A. Skjellum, *Using MPI* (MIT Press, Cambridge, MA, 1999), 2nd ed.
- ²³See <http://sprng.cs.fsu.edu>
- ²⁴D. P. Belanger, P. Norblad, A. R. King, V. Jaccarino, L. Lundgren, and O. Beckman, *J. Magn. Magn. Mater.* **31-34**, 1095 (1983).
- ²⁵P. J. van der Zaag, Y. Ijiri, J. A. Borchers, L. F. Feiner, R. M. Wolf, J. M. Gaines, R. W. Erwin, and M. A. Verheijen, *Phys. Rev. Lett.* **84**, 6102 (2000).
- ²⁶H. Shi, D. Lederman, N. R. Dilley, R. C. Black, J. Diedrichs, K. Jensen, and M. B. Simmonds, *J. Appl. Phys.* **93**, 8600 (2003).
- ²⁷S. Chikazumi, *Physics of Magnetism* (Wiley, New York, 1964), p. 137.
- ²⁸J. C. Slonczewski, *Phys. Rev. Lett.* **67**, 3172 (1991).
- ²⁹M. Kiwi, J. Mejía-López, R. D. Portugal, and R. Ramírez, *Europhys. Lett.* **48**, 573 (1999).
- ³⁰M. Kiwi, J. Mejía-López, R. D. Portugal, and R. Ramírez, *Appl. Phys. Lett.* **75**, 3995 (1999).